

## Al-Mg systematics of hibonite-bearing Ca,Al-rich inclusions from Ningqiang

Weibiao HSU<sup>1,2\*</sup>, Yunbin GUAN<sup>3</sup>, and Ying WANG<sup>1</sup>

<sup>1</sup>Purple Mountain Observatory, Nanjing 210008, China

<sup>2</sup>State Key Laboratory of Geological Processes and Mineral Resources and Faculty of Earth Sciences, China University of Geosciences, Wuhan 430047, China

<sup>3</sup>Division of Geological and Planetary Sciences, California Institute of Technology, Pasadena, California 91125, USA

\*Corresponding author. E-mail: wbxu@pmo.ac.cn

(Received 12 September 2010; revision accepted 07 January 2011)

**Abstract**—Hibonite-bearing Ca,Al-rich inclusions (CAIs) usually occur in CM and CH chondrites and possess petrographic and isotopic characteristics distinctive from other typical CAIs. Despite their highly refractory nature, most hibonite-bearing CAIs have little or no <sup>26</sup>Mg excess (the decay product of <sup>26</sup>Al), but do show wide variations of Ca and Ti isotopic anomalies. A few spinel-hibonite spherules preserve evidence of live <sup>26</sup>Al with an inferred <sup>26</sup>Al/<sup>27</sup>Al close to the canonical value. The bimodal distribution of <sup>26</sup>Al abundances in hibonite-bearing CAIs has inspired several interpretations regarding the origin of short-lived nuclides and the evolution of the solar nebula. Herein we show that hibonite-bearing CAIs from Ningqiang, an ungrouped carbonaceous chondrite, also provide evidence for a bimodal distribution of <sup>26</sup>Al. Two hibonite aggregates and two hibonite-pyroxene spherules show no <sup>26</sup>Mg excesses, corresponding to inferred <sup>26</sup>Al/<sup>27</sup>Al < 8 × 10<sup>-6</sup>. Two hibonite-melilite spherules are indistinguishable from each other in terms of chemistry and mineralogy but have different Mg isotopic compositions. Hibonite and melilite in one of them display positive <sup>26</sup>Mg excesses (up to 25‰) that are correlated with Al/Mg with an inferred <sup>26</sup>Al/<sup>27</sup>Al of (5.5 ± 0.6) × 10<sup>-5</sup>. The other one contains normal Mg isotopes with an inferred <sup>26</sup>Al/<sup>27</sup>Al < 3.4 × 10<sup>-6</sup>. Hibonite in a hibonite-spinel fragment displays large <sup>26</sup>Mg excesses (up to 38‰) that correlate with Al/Mg, with an inferred <sup>26</sup>Al/<sup>27</sup>Al of (4.5 ± 0.8) × 10<sup>-5</sup>. Prolonged formation duration and thermal alteration of hibonite-bearing CAIs seem to be inconsistent with petrological and isotopic observations of Ningqiang. Our results support the theory of formation of <sup>26</sup>Al-free/poor hibonite-bearing CAIs prior to the injection of <sup>26</sup>Al into the solar nebula from a nearby stellar source.

### INTRODUCTION

Ca,Al-rich inclusions (CAIs) in chondritic meteorites are the most primitive and oldest objects formed in the early solar system (Amelin et al. 2002; MacPherson 2003). They are composed of refractory minerals thought to be the first phases condensed from a solar gas during cooling from very high temperatures (Grossman 1972). The most common phases present in CAIs of CV chondrites are melilite, spinel, Ti,Al-rich calcic pyroxene, and anorthite. A few CAIs contain hibonite (CaAl<sub>12</sub>O<sub>19</sub>), an ultra refractory mineral. Hibonite-bearing CAIs most commonly occur in CM and CH chondrites and possess petrographic and

isotopic characteristics distinctive from other CAIs (Hinton et al. 1988; Ireland 1988; Krot et al. 2002, 2008; Liu et al. 2009; Zhang and Hsu 2009). Hibonite occurs as single, isolated crystals in the matrix; as aggregates of plates and fragments; in dense spherules of hibonite and spinel; and in hibonite-silicate spherules. Most hibonite-bearing CAIs are essentially devoid of <sup>26</sup>Al but preserve large stable isotope (e.g., Ca and Ti) anomalies (Ireland 1988; Liu et al. 2009). A few spinel-hibonite spherules preserve evidence of in situ decay of <sup>26</sup>Al with an inferred initial <sup>26</sup>Al/<sup>27</sup>Al close to the canonical value, but these spherules lack large Ca and Ti isotopic anomalies. Apparently, as summarized by MacPherson (2003), <sup>50</sup>Ti and <sup>48</sup>Ca isotope anomalies

and evidence for  $^{26}\text{Al}$  decay are mutually exclusive in hibonite-rich CAIs.

Evidence of live  $^{26}\text{Al}$  has been found in a variety of CAIs and chondrules (Lee et al. 1977; Hutcheon and Hutchison 1989; MacPherson et al. 1995; Guan et al. 2000, 2006; Hsu et al. 2000, 2003; Kita et al. 2000; Krot et al. 2008; Villeneuve et al. 2009). The initial  $^{26}\text{Al}/^{27}\text{Al}$  of the solar system is close to  $5 \times 10^{-5}$ . The Al-Mg system can potentially serve as a high resolution chronometer for events that occurred within the first few million years of solar system history if  $^{26}\text{Al}$  was homogeneously distributed (Hsu et al. 2000; Villeneuve et al. 2009). The bimodal distribution of  $^{26}\text{Al}$  abundances in hibonite-bearing CAIs casts a serious challenge to the use of  $^{26}\text{Al}$  as a precise chronometer for early solar system events. It is not clear whether such a difference reflects a prolonged duration of CAI formation or implies local heterogeneity of  $^{26}\text{Al}$  distribution in the nebula.

Ningqiang is an ungrouped carbonaceous chondrite (Wang and Hsu 2009). It shares many chemical and petrologic characteristics with CV and CK chondrites. About 7% of the CAIs in Ningqiang are hibonite-bearing. In contrast, most CAIs in CV and CK chondrites do not contain hibonite. Hibonite, if present, is a minor component in CAIs of CV and CK chondrites. Hibonite-bearing CAIs in Ningqiang exhibit a variety of petrographic textures: aggregates of euhedral hibonite crystals; fragments of hibonite in matrix; hibonite-spinel, hibonite-melilite, and hibonite-pyroxene spherules. As a part of an on-going project, we carried out an extensive petrologic and magnesium isotopic study of hibonite-bearing CAIs from Ningqiang. We use these results to shed some new light on the origin and distribution of  $^{26}\text{Al}$  in the early solar system.

## EXPERIMENTS

One-inch round thick and thin sections of Ningqiang were examined with a Nikon E400 POL optical microscope and a Hitachi S-3400N scanning electron microscope (SEM) equipped with an OXFORD INCA7021 energy dispersive spectroscopy (EDS) system. To search for refractory inclusions, automatic X-ray mapping analyses were performed on each section with a resolution of 2–5  $\mu\text{m}$  per pixel.

In situ chemical analyses were made with electron microprobes (EMPs) at China University of Geosciences, Wuhan (JEOL JXA-8100M) and Nanjing University (JEOL JXA-8800M). Working conditions are as follows: 15 kV accelerating voltage, 20 nA beam current, and a focused beam. Both synthetic and natural mineral standards were used. ZAF corrections were applied.

Mg isotopes and Al/Mg ratios were analyzed with the Cameca Geq-7f ion microprobe at Caltech, using an  $\text{O}^-$  primary beam. The details of the method were described by Fahey et al. (1987). A mass resolution of 3000 was used, which is sufficient to remove hydride and other interferences. Measurements were carried out through the mass sequence 24, 25, 26, and 27. Each analysis is an average of 50–100 cycles through the above mass sequence. Standards of Burma spinel, San Carlos olivine, melilite glass, and magnesium metal were analyzed before and after measurements. A beam current of 0.2–0.3 nA was used to keep the count rate of  $^{24}\text{Mg}$  under  $10^5 \text{ s}^{-1}$ .

The goal was to look for  $^{26}\text{Mg}$  excesses due to the decay of  $^{26}\text{Al}$ . A linear law was assumed for the Mg isotope mass fractionation, and the mass-fractionation-corrected, nonlinear  $^{26}\text{Mg}$  excess was calculated using the following equation

$$\delta^{26}\text{Mg} = \Delta^{26}\text{Mg} - 2 \times \Delta^{25}\text{Mg} \quad (1)$$

where

$$\Delta^{25}\text{Mg} = \left[ \frac{[^{25}\text{Mg}^+ / ^{24}\text{Mg}^+]_{\text{MEAS}}}{[^{25}\text{Mg} / ^{24}\text{Mg}]_{\text{REF}}} - 1 \right] \times 1000 (\text{‰})$$

$$\Delta^{26}\text{Mg} = \left[ \frac{[^{26}\text{Mg}^+ / ^{24}\text{Mg}^+]_{\text{MEAS}}}{[^{26}\text{Mg} / ^{24}\text{Mg}]_{\text{REF}}} - 1 \right] \times 1000 (\text{‰})$$

where

$$[^{26}\text{Mg} / ^{24}\text{Mg}]_{\text{REF}} = 0.13932$$

and

$$[^{25}\text{Mg} / ^{24}\text{Mg}]_{\text{REF}} = 0.12663$$

(Catanzaro et al. 1966).

## RESULTS

A total of 294 CAIs were found in six polished thick sections and nine polished thin sections of Ningqiang. Among them, 22 contain hibonite. They range in size from about 20 to 400  $\mu\text{m}$  and exhibit a variety of petrographic textures. For practical reasons, we studied the CAIs with hibonite crystals larger than 5  $\mu\text{m}$ . They are (1) aggregates of euhedral hibonite plates in matrix (Fig. 1a) or mantled by multilayered rims (Fig. 1b), (2) euhedral hibonite crystals or fragments in matrix (Fig. 1c), (3) hibonite and aluminous pyroxene spherules (Figs. 1d and 1e), (4) hibonite and melilite + perovskite inclusions (Figs. 1f and 1g), (5) hibonite-spinel fragment (Fig. 1h).

One hibonite aggregate (PMO-0025 CAI 6, Fig. 1a) is composed of large euhedral hibonite plates (up to

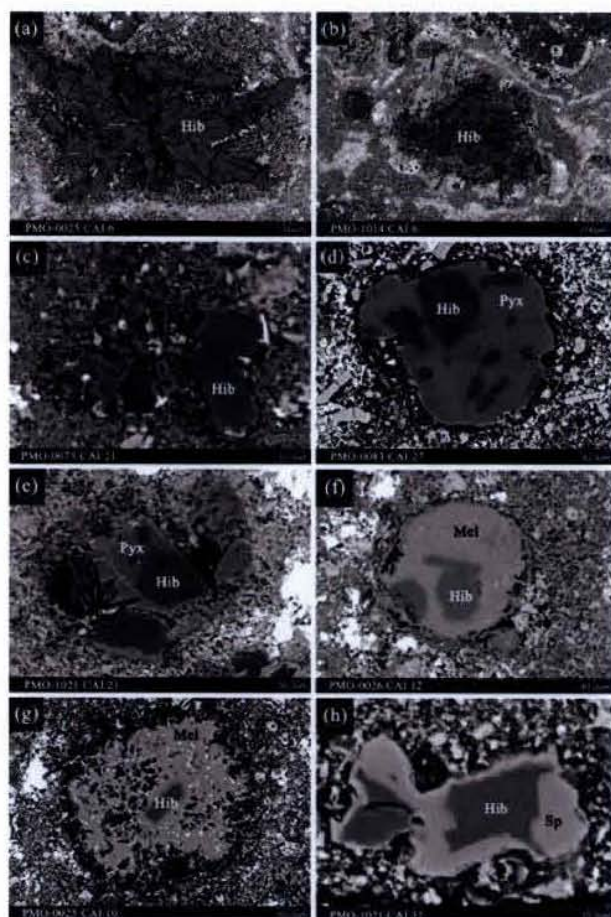


Fig. 1. Petrographic occurrences of hibonite-bearing CAIs in Ningqiang: a) Aggregates of euhedral hibonite plates in matrix or b) mantled by multilayered rims. c) Euhedral hibonite crystals or fragments in matrix. d) and e) Hibonite and aluminous pyroxene spherules. f) and g) Hibonite and melilite + perovskite inclusions. h) Hibonite-spinel fragment. Hib, hibonite; Pyx, pyroxene; Sp, spinel; Mel, melilite. Perovskite is highly reflective phase included in melilite.

200  $\mu\text{m}$  in length). The plates are oriented radially. Small perovskite (submicron) grains occur interstitially between hibonite grains. The other (PMO-1014 CAI 6, Fig. 1b) is enclosed by a high-Al pyroxene rim and a fayalite rim. Perovskite, high-Al pyroxene, melilite, and secondary phases (sodalite and hedenbergite) occur interstitially between hibonite crystals in this CAI. In PMO-0083 CAI 27 (Fig. 1d), euhedral hibonite plates are set in a high-Al,Ti pyroxene (similar in composition to fassaite). Small grains (micron-size) of melilite and spinel are also present in the hibonite-pyroxene spherule (PMO-1021 CAI 21, Fig. 1e). Euhedral hibonite crystals are set in melilite peppered with submicron perovskite grains in both hibonite-melilite spherules. One (PMO-0026 CAI 12, Fig. 1f) is compact, and the other (PMO-0025

CAI 10, Fig. 1g) is porous. The hibonite-spinel fragment (PMO-1021 CAI 32, Fig. 1h) is similar in texture to SHIBs (Spinel-HIBonite spherules; Ireland 1988).

Representative mineral compositions of hibonite-bearing CAIs from Ningqiang are presented in Table 1. Hibonite shows substantial chemical variations with MgO and TiO<sub>2</sub> concentrations ranging from 0.33 to 3.40 wt% and 0.52 to 7.39%, respectively. The content of Al varies inversely with that of Ti + Mg, indicating a coupled substitution of  $\text{Ti}^{4+} + \text{Mg}^{2+} = 2\text{Al}^{3+}$  (Fig. 2). Aggregated euhedral hibonite crystals show a restricted range and relatively low MgO and TiO<sub>2</sub> contents from 0.4 to 1.1% and 1.0 to 2.2%, respectively. In contrast, hibonite in hibonite-melilite CAIs is characterized by a wide range of MgO and TiO<sub>2</sub> concentrations, 0.3–3.4% and 0.5–7.4%, respectively (Fig. 2). Hibonite in hibonite-pyroxene spherules and in matrix has similar compositions to those of euhedral hibonite aggregates. Hibonite in hibonite-spinel fragments has intermediate contents of MgO (0.9–2.4%) and TiO<sub>2</sub> (1.8–4.0%). Melilite is Al-rich and in the range of  $\text{Ak}_{0.2-10.7}$  with an average of  $\text{Ak}_{3.2}$ . Spinel in hibonite-melilite CAIs has a much higher Mg# (molar  $\text{Mg}/[\text{Mg} + \text{Fe}]$ , 98) than that in hibonite-spinel fragment (51) and that in hibonite-pyroxene CAIs (44). Pyroxene in hibonite-pyroxene spherules is highly enriched in Al and Ti, with Al<sub>2</sub>O<sub>3</sub> and TiO<sub>2</sub> contents up to 31.9 wt% and 5.4 wt%, respectively. However, pyroxene in CAI rims contains much less Al<sub>2</sub>O<sub>3</sub> (0.1–15.2 wt%) and TiO<sub>2</sub> (0–0.4 wt%). This is similar to that found in Wark-Lovering rims.

Mg isotopic compositions were analyzed in seven hibonite-bearing CAIs: two hibonite aggregates, two hibonite-pyroxene spherules, two hibonite-melilite spherules, and one hibonite-spinel fragment (Fig. 3, Table 2). Hibonite and melilite have relatively high but variable <sup>27</sup>Al/<sup>24</sup>Mg ratios (up to 195 and 28, respectively). Within the analytical uncertainty, hibonite in two hibonite aggregates (PMO-0025 CAI 6 and PMO-1014 CAI 6) and two hibonite-pyroxene spherules (PMO-0083 CAI 27 and PMO-1021 CAI 21) has normal Mg isotopic compositions relative to terrestrial standards. Their inferred <sup>26</sup>Al/<sup>27</sup>Al ratios are  $< 8 \times 10^{-6}$ . Two hibonite-melilite spherules show distinctively different Mg isotopic compositions. Hibonite and melilite in one CAI (PMO-0026 CAI 12) reveal positive <sup>26</sup>Mg excesses (up to 25‰) which are well correlated with Al/Mg. The inferred initial <sup>26</sup>Al/<sup>27</sup>Al is  $(5.5 \pm 0.6) \times 10^{-5}$ , essentially the same as the canonical value. The other one (PMO-0025 CAI 10) contains normal Mg isotopic compositions. The inferred <sup>26</sup>Al/<sup>27</sup>Al is  $< 3.4 \times 10^{-6}$ . Hibonite in the hibonite-spinel fragment (PMO-1021 CAI 32) displays large

Table 1. Average and representative compositions (wt%) of minerals in hibonite-bearing CAIs from Ningqiang.

Phases	Hib aggregates (2 <sup>a</sup> )				Hib + Mel ( $\pm$ Sp $\pm$ Prv) (7 <sup>a</sup> )				Hib + Sp (2 <sup>a</sup> )		Hib + Al,Ti-Di ( $\pm$ Sp) (2 <sup>a</sup> )			Hib fragments (4 <sup>a</sup> )	
	Hib ( $\pm$ 1 $\sigma$ , 14 <sup>b</sup> )	Mel <sup>c</sup>	Di <sup>c</sup>	Fa <sup>c</sup>	Hib (8 <sup>b</sup> )	Mel	Sp	Prv	Al-Di <sup>c</sup>	Hib (3 <sup>b</sup> )	Sp	Hib (2 <sup>b</sup> )	Al,Ti-Di	Sp	Hib (4 <sup>b</sup> )
CaO	8.72 $\pm$ 0.35	40.2	25.6	0.39	9.11 $\pm$ 0.96	40.1	0.13	40.0	23.8	8.31 $\pm$ 0.27	0.37	9.55 $\pm$ 0.06	24.7	0.41	8.79 $\pm$ 0.52
TiO <sub>2</sub>	1.76 $\pm$ 0.30	0.12	nd	0.04	3.47 $\pm$ 2.43	0.09	0.15	57.4	0.15	2.97 $\pm$ 1.10	0.26	1.62 $\pm$ 0.35	3.88	0.74	1.61 $\pm$ 0.47
Al <sub>2</sub> O <sub>3</sub>	88.2 $\pm$ 0.60	33.4	0.09	0.84	84.7 $\pm$ 3.42	36.0	71.5	1.27	15.2	84.8 $\pm$ 0.79	65.7	86.4 $\pm$ 0.21	31.9	64.0	87.5 $\pm$ 0.96
MgO	0.82 $\pm$ 0.15	1.07	18.2	22.6	1.94 $\pm$ 1.22	0.55	26.3	nd	13.8	1.56 $\pm$ 0.74	13.6	0.90 $\pm$ 0.15	4.91	10.5	0.76 $\pm$ 0.08
SiO <sub>2</sub>	nd	23.9	55.1	34.8	0.26 $\pm$ 0.18	22.5	0.02	0.74	45.2	0.32 $\pm$ 0.40	0.46	1.04 $\pm$ 1.14	33.5	0.34	0.38 $\pm$ 0.64
FeO	0.24 $\pm$ 0.06	0.57	0.72	41.2	0.48 $\pm$ 0.22	0.71	1.14	0.14	1.08	1.01 $\pm$ 0.92	19.6	0.23 $\pm$ 0.10	0.22	23.3	0.76 $\pm$ 0.33
Na <sub>2</sub> O	nd	0.33	nd	0.07	nd	0.08	nd	0.03	0.05	nd	0.03	nd	nd	nd	nd
Cr <sub>2</sub> O <sub>3</sub>	nd	nd	nd	0.10	0.03 $\pm$ 0.02	0.03	0.02	0.02	nd	nd	0.09	nd	nd	0.08	nd
Total	99.8 $\pm$ 0.53	99.6	99.7	100.0	100.0 $\pm$ 0.65	100.1	99.3	99.6	99.3	99.0 $\pm$ 1.04	100.1	99.7 $\pm$ 1.55	99.1	99.4	99.8 $\pm$ 0.57

<sup>a</sup>Number of CAIs analyzed.<sup>b</sup>Number of analyses.<sup>c</sup>Phases in rims surrounding host CAIs.

Hib = hibonite; Mel = melilite; Di = diopside; Fa = fayalitic olivine; Sp = spinel; Prv = perovskite; nd = not detected.

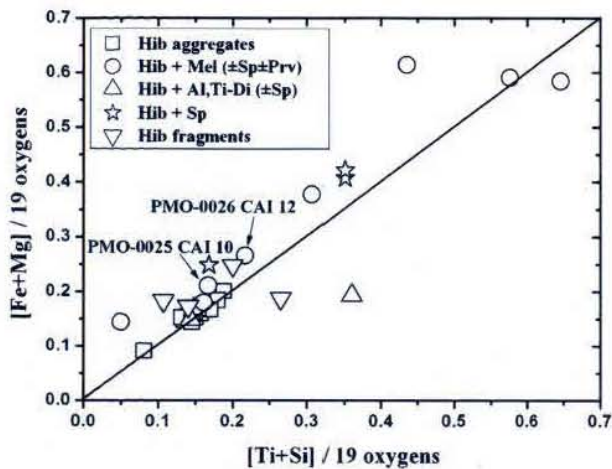


Fig. 2. Chemical compositions of hibonite in Ningqiang, plotted in terms of cations per formula unit (19 cations). Hibonites in hibonite-melilite spherules (arrowed) analyzed by SIMS in this work have very similar compositions.

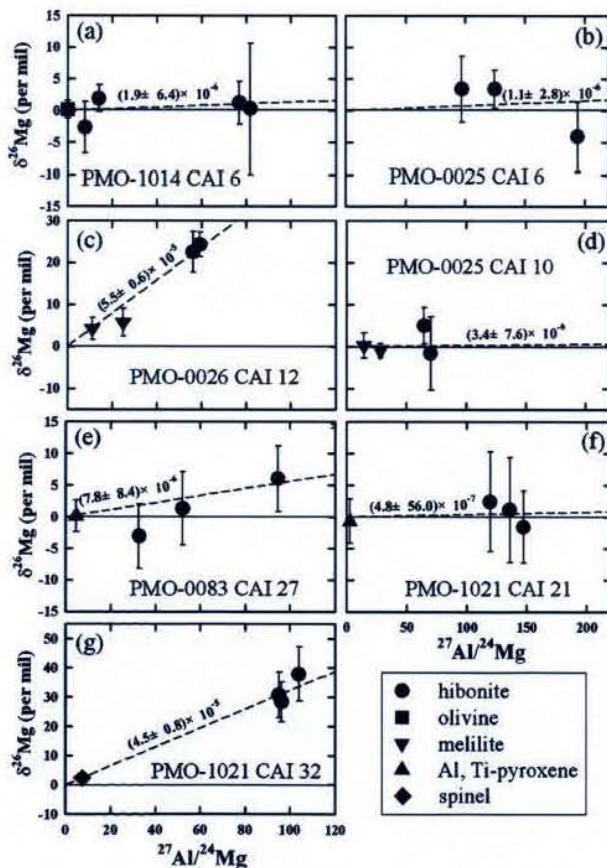


Fig. 3. Al-Mg systematics of hibonite-bearing CAIs in Ningqiang. They show a bimodal  $^{26}\text{Al}$  distribution, with the majority being  $^{26}\text{Al}$ -free/poor.

Table 2. Mg isotopes and inferred  $^{26}\text{Al}/^{27}\text{Al}$  of hibonite-bearing CAIs from Ningqiang.

	$^{27}\text{Al}/^{24}\text{Mg} \pm 2\sigma$	$\delta^{26}\text{Mg} \pm 2\sigma$
PMO-0025 CAI 6 ( $^{26}\text{Al}/^{27}\text{Al}$ ) = $(1.1 \pm 2.8) \times 10^{-6}$		
Hibonite	$97.0 \pm 1.6$	$3.4 \pm 5.2$
Hibonite	$194.3 \pm 0.4$	$-4.1 \pm 5.5$
Hibonite	$124.4 \pm 0.2$	$3.4 \pm 3.0$
PMO-0025 CAI 10 ( $^{26}\text{Al}/^{27}\text{Al}$ ) = $(3.4 \pm 7.6) \times 10^{-6}$		
Melilite	$14.6 \pm 0.1$	$0.2 \pm 3.0$
Melilite	$28.3 \pm 0.1$	$-1.0 \pm 1.7$
Hibonite	$65.0 \pm 0.1$	$5.0 \pm 4.3$
Hibonite	$70.6 \pm 0.2$	$-1.6 \pm 8.7$
PMO-0026 CAI 12 ( $^{26}\text{Al}/^{27}\text{Al}$ ) = $(5.5 \pm 0.6) \times 10^{-5}$		
Hibonite	$59.3 \pm 0.1$	$24.3 \pm 2.9$
Hibonite	$56.3 \pm 0.1$	$22.5 \pm 4.9$
Melilite	$11.1 \pm 0.1$	$4.2 \pm 2.6$
Melilite	$25.1 \pm 0.1$	$5.7 \pm 3.3$
PMO-0083 CAI 27 ( $^{26}\text{Al}/^{27}\text{Al}$ ) = $(7.8 \pm 8.4) \times 10^{-6}$		
Hibonite	$94.8 \pm 0.3$	$6.0 \pm 5.2$
Hibonite	$52.2 \pm 1.8$	$1.3 \pm 5.8$
Hibonite	$32.8 \pm 0.9$	$-3.1 \pm 5.1$
High-Al pyroxene	$4.6 \pm 0.1$	$0.1 \pm 2.5$
PMO-1014 CAI 6 ( $^{26}\text{Al}/^{27}\text{Al}$ ) = $(1.9 \pm 6.4) \times 10^{-4}$		
Olivine	$<0.01$	$0.2 \pm 1.4$
Hibonite	$82.0 \pm 0.2$	$0.3 \pm 10.3$
Hibonite	$7.8 \pm 0.1$	$-2.7 \pm 4.1$
Hibonite	$14.2 \pm 0.1$	$1.9 \pm 2.1$
Hibonite	$77.0 \pm 0.1$	$1.2 \pm 3.4$
PMO-1021 CAI 21 ( $^{26}\text{Al}/^{27}\text{Al}$ ) = $(4.8 \pm 56.0) \times 10^{-7}$		
Hibonite	$147.4 \pm 0.3$	$-1.6 \pm 5.7$
Hibonite	$135.7 \pm 1.2$	$1.1 \pm 8.3$
Hibonite	$119.5 \pm 1.2$	$2.4 \pm 7.9$
High-Al pyroxene	$2.6 \pm 0.1$	$-0.7 \pm 3.5$
PMO-1021 CAI 32 ( $^{26}\text{Al}/^{27}\text{Al}$ ) = $(4.5 \pm 0.8) \times 10^{-5}$		
Hibonite	$104.2 \pm 0.5$	$37.9 \pm 9.3$
Hibonite	$96.4 \pm 0.4$	$28.4 \pm 6.8$
Hibonite	$95.3 \pm 0.8$	$30.8 \pm 7.8$
Spinel	$7.4 \pm 0.1$	$2.4 \pm 1.9$

well-resolved  $^{26}\text{Mg}$  excesses (up to 38‰), correlated with Al/Mg. The inferred initial  $^{26}\text{Al}/^{27}\text{Al}$  is  $(4.5 \pm 0.8) \times 10^{-5}$ , close to the canonical value.

## DISCUSSION

Previous studies revealed that hibonite-bearing CAIs display correlated morphological, chemical, and isotopic characteristics (Ireland 1988, 1990; Liu et al. 2009). PLAty crystal fragments (PLACs) and Blue AGgregates (BAGs) generally have little or no  $^{26}\text{Mg}$  excess (radiogenic), but wide variations of Ca and Ti isotopic compositions (i.e.,  $\delta^{50}\text{Ti}$  from  $-80$  to  $+273\%$ ). Almost all spinel-hibonite spherules (SHIBs) have excess  $^{26}\text{Mg}$  that is correlated with Al/Mg. The inferred  $^{26}\text{Al}/^{27}\text{Al}$  for SHIBs is  $4.5 \times 10^{-5}$  (Liu et al. 2009). SHIBs usually have small ( $<10\%$ ) Ca- and Ti-isotopic

anomalies. Hibonite-pyroxene spherules from CO and CM chondrites have no radiogenic  $^{26}\text{Mg}$  or slight depletion of  $^{26}\text{Mg}$  (about  $-3\%$  on average) but resolved excesses or depletions of  $^{48}\text{Ca}$  ( $-45$  to  $40\%$ ) and  $^{50}\text{Ti}$  ( $-60$  to  $+100\%$ ) (Ireland et al. 1991; Russell et al. 1998; Simon et al. 1998). A hibonite-pyroxene spherule from an EH3 chondrite has a negligible  $^{26}\text{Mg}$  excess (Guan et al. 2000). One hibonite-pyroxene CAI in Acfer 214 (CH) is also essentially free of live  $^{26}\text{Al}$  (Krot et al. 2008). Hibonite-melilite CAIs usually occur in CH chondrites (Krot et al. 2002; Zhang and Hsu 2009). They show either unresolvable or small  $^{26}\text{Mg}$  excesses corresponding to an initial  $^{26}\text{Al}/^{27}\text{Al}$  of  $4 \times 10^{-7}$  (Krot et al. 2008). Hibonite-bearing type A CAIs in CV chondrites display well-correlated  $^{26}\text{Mg}$  excesses with a canonical or supracanonical  $^{26}\text{Al}/^{27}\text{Al}$  ratio (Cosarinsky et al. 2006).

Our new data on the petrology and magnesium isotopes of hibonite-bearing CAIs in Ningqiang confirm and extend previous results. These refractory inclusions show similar petrological and isotopic characteristics with those of CM, CO, and CH chondrites. Hibonite aggregates and hibonite-pyroxene spherules in Ningqiang have little or no  $^{26}\text{Mg}$  excesses; whereas the hibonite-spinel fragment exhibits a large well-resolved  $^{26}\text{Mg}$  excess corresponding to an initial  $^{26}\text{Al}/^{27}\text{Al}$  close to the canonical value. One hibonite-melilite CAI is essentially free of live  $^{26}\text{Al}$ , consistent with the previous findings. But the other displays large  $^{26}\text{Mg}$  excesses with an inferred  $^{26}\text{Al}/^{27}\text{Al}$  of  $5.5 \times 10^{-5}$ , similar to the hibonite-bearing type A CAIs in CV chondrites. The  $^{26}\text{Al}$ -rich and  $^{26}\text{Al}$ -free hibonite-melilite CAIs in Ningqiang are chemically and mineralogically indistinguishable (Figs. 1 and 2).

It is evident that hibonite-bearing CAIs in Ningqiang display a bimodal distribution of live  $^{26}\text{Al}$  in the early solar system. These observations can be interpreted as (1) prolonged formation duration of hibonite-bearing CAIs; (2) thermal alteration of Al-Mg systematics of hibonite-bearing CAIs on their chondrite parent body or in the nebula; (3) local heterogeneity of  $^{26}\text{Al}$  distribution in the early solar system; (4) formation of  $^{26}\text{Al}$ -free/poor hibonite-bearing CAIs prior to the injection and homogenization of  $^{26}\text{Al}$  in the protoplanetary disk.

$^{26}\text{Al}$ - $^{26}\text{Mg}$  isotope systematics potentially provides constraints on the relative timing of events that occurred during the early stages of solar system formation (Villeneuve et al. 2009). In principle, objects formed at the very beginning (time zero) of the solar system would have a canonical  $^{26}\text{Al}$  abundance.  $^{26}\text{Al}$ -free/poor CAIs would have formed later. If we assume that  $^{26}\text{Al}$  was homogeneously distributed in the early solar nebula, the formation interval for the two hibonite-melilite CAIs in

Ningqiang will be more than 2.9 Myr, and the formation duration for  $^{26}\text{Al}$ -rich and  $^{26}\text{Al}$ -free hibonite-bearing CAIs in Ningqiang will be even longer ( $>5$  Myr). Such a prolonged duration faces several critical challenges with regard to the evolution of solar nebula. It is known that the rate of sweeping out of small objects ( $<1$  m) into the protosun due to gas drag during the nebular accretion phase is rapid (time scale of about  $10^5$  yr; Weidenschilling and Cuzzi 1993). A recent study argued that the duration of the solar nebula could be longer (about  $10^6$  yr) due to vertical motions of dust grains in a turbulent protoplanetary disk (Ciesla 2010). But it is still difficult to envision that  $^{26}\text{Al}$ -rich and  $^{26}\text{Al}$ -poor hibonite-bearing CAIs could form in the nebula over an extended time (several Myr). Overwhelming evidence from short-lived and long-lived isotope analyses shows that CAIs formed within a very brief formation interval at the early stage of solar nebula (Hsu et al. 2000; Amelin et al. 2002; Thrane et al. 2006; Jacobsen et al. 2008). The prolonged formation duration also appears to be inconsistent with stable isotope anomalies (i.e., Ca and Ti) observed in hibonite-bearing CAIs. The anomalous compositions have been interpreted as signatures of distinct nucleosynthetic components that contributed to the solar nebula (Zinner et al. 1986). Isotopic anomalies were shortly (on a time scale of  $10^5$  yr) obliterated by continued mixing during the nebular accretion process (Ouellette et al. 2009). It is difficult to retain large isotopic anomalies for several million years after the formation of typical CAIs whose isotopes already had been well homogenized. The late formation model is also inconsistent with the observation that  $^{26}\text{Al}$ -free/poor hibonite-bearing CAIs are usually  $^{16}\text{O}$ -rich (Krot et al. 2008; Liu et al. 2009). The current understanding of oxygen isotope evolution in the early solar system suggests that the inner solar nebula was initially  $^{16}\text{O}$ -rich ( $\Delta^{17}\text{O} \sim -25\%$ ) and evolved toward  $^{16}\text{O}$ -poor on a short time scale (0.5–1 Myr) (Yurimoto and Kuramoto 2004; Krot et al. 2005; Lyons and Young 2005; Lyons et al. 2009; Makide et al. 2009).

Chondritic meteorites experienced different degrees of thermal processing on their parent bodies, including thermal and shock metamorphism, aqueous and hydrothermal alteration. Thermal diffusion of Mg took place during these processes (LaTourrette and Wasserburg 1998; LaTourrette and Hutcheon 1999). The preponderance of evidence shows that  $^{26}\text{Al}$ - $^{26}\text{Mg}$  system was partly or completely reset in chondrites of petrological type 3.5 and above (Kita et al. 2000; Huss et al. 2001). Therefore, the apparent extended time interval may just reflect the planetary processes. But, petrological and isotopic studies indicate that Ningqiang only experienced a mild degree of thermal

metamorphism (Guimon et al. 1995; Kimura et al. 1997; Hsu et al. 2003; Wang and Hsu 2009). The peak temperature did not exceed 300 °C on its parent body. In this temperature range, magnesium isotopes in hibonite-bearing CAIs would not equilibrate with Mg rich phases over the age of the solar system. It is possible that  $^{26}\text{Al}$ -free/poor hibonite-bearing CAIs of Ningqiang could have been affected by thermal processes in the solar nebula such as lightning, shock waves, reheating/remelting by gas drag, etc., prior to accretion into their parent body. Evidence of nebular processing is reflected in the abundances and characteristics of presolar components among the classes of carbonaceous chondrites (Huss et al. 2003). However, the correlated morphological, chemical, and isotopic characteristics observed in hibonite-bearing CAIs of Ningqiang as well as other carbonaceous chondrites make such an interpretation less attractive. It would be very difficult to account for the preservation of large isotopic anomalies (i.e.,  $\delta^{50}\text{Ti}$  from  $-80$  to  $+273\%$ ) in  $^{26}\text{Al}$ -free/poor hibonite-bearing CAIs. In fact, the compact hibonite-melilite spherule (PMO-0026 CAI 12, Fig. 1f) in Ningqiang seems to have experienced remelting and recrystallization processes in the nebula, yet it still retains the evidence of in situ  $^{26}\text{Al}$  decay.

In general, short-lived radionuclides can be produced either by irradiation of dust and gas with an intense flux of cosmic rays or energetic particles (Lee et al. 1998; Gounelle et al. 2001) or by thermal nucleosynthesis in the interiors of stars (Cameron et al. 1995; Busso et al. 2003; Wasserburg et al. 2006). If  $^{26}\text{Al}$  was made locally by spallation reactions with energetic particles from an active young Sun, then it is likely that  $^{26}\text{Al}$  would not be distributed uniformly throughout the accretion disk.  $^{26}\text{Al}$ -rich and  $^{26}\text{Al}$ -free CAIs could have formed contemporaneously in spatially distinct regions in the solar nebula. In that case, the observed differences in their  $^{26}\text{Al}/^{27}\text{Al}$  ratios would reflect variable local formation of  $^{26}\text{Al}$  by energetic particle irradiation and would not have any chronological implications. A special case has been postulated that CAIs and chondrules were produced in the reconnection ring close to the proto-Sun where they were heated repeatedly by intense impulsive flares before being lifted up by an outflowing X-wind and falling onto planetary surfaces all over the solar system (Shu et al. 1996, 1997). According to this scenario,  $^{26}\text{Al}$ -rich CAIs were produced in a region closer to the proto-Sun and experienced a longer exposure time to impulsive flares in the reconnection ring than  $^{26}\text{Al}$ -poor/free CAIs and chondrules (Lee et al. 1998). Because the inner part of the reconnection ring has high temperatures and high flux of energetic particles, different nucleosynthetic

components were completely homogenized and short-lived nuclides were synthesized in typical CAIs. In contrast,  $^{26}\text{Al}$ -poor/free CAIs were heated for a shorter period and exposed to less intense flares and thus contained almost no  $^{26}\text{Al}$  but did retain large anomalies of stable isotopes (Lee et al. 1998; Lee and Shen 2001). The irradiation model avoids many difficulties inherent to other models but unfortunately has its own problems. It is inconsistent with the high degree of uniformity of initial  $^{26}\text{Al}/^{27}\text{Al}$  inferred for typical CAIs (the so-called canonical value), since an irradiation process would produce a wider range of initial ratios than the narrow one observed. The underproduction of  $^{26}\text{Al}$  by a factor of 20 relative to  $^{41}\text{Ca}$  on the basis of inferred irradiation yields is another serious problem (Lee et al. 1998; Sahijpal and Gupta 2009). The presence of  $^{10}\text{Be}$ , a spallation-generated, short-lived radionuclide, coupled with the absence of  $^{41}\text{Ca}$  and  $^{26}\text{Al}$  in some hibonite-bearing CAIs further weakens the likelihood of energetic particle irradiation in the production of short-lived radionuclides present in primitive meteorites (Marhas et al. 2002). The close correlation (simultaneous presence or absence) between initial abundances of  $^{41}\text{Ca}$  and  $^{26}\text{Al}$  in hibonite-bearing CAIs implies a stellar origin for the short-lived radionuclides (Sahijpal et al. 1998). The age difference (about 2 Myr) between the formation of typical CAIs and chondrules, determined using the U-Pb system, is in excellent agreement with relative ages inferred from the  $^{26}\text{Al}$ - $^{26}\text{Mg}$  clock, strongly supporting a stellar origin for  $^{26}\text{Al}$  (Amelin et al. 2002; Connelly et al. 2008).

If  $^{26}\text{Al}$  has a stellar origin, then a late injection into the protoplanetary disk from nearby stars is required because the initial  $^{26}\text{Al}/^{27}\text{Al}$  ( $5 \times 10^{-5}$ ) inferred for primitive meteorites is much higher than the average  $^{26}\text{Al}/^{27}\text{Al}$  ( $1 \times 10^{-5}$ ) in the galactic background based on gamma ray observations (Mahoney et al. 1984). Injection of freshly synthesized short-lived radionuclides from a stellar source into the protosolar molecular cloud could also trigger its gravitational collapse, leading to the formation of the solar system (Cameron and Truran 1977; Boss and Vanhala 2000). Detailed studies suggest that injection of short-lived nuclides into the central zone of the collapsing cloud will not be instantaneous, and it may take more than  $(2-4) \times 10^5$  yr following the impact (Foster and Boss 1997). It has been suggested that  $^{26}\text{Al}$ -free/poor refractory inclusions, such as hibonite-bearing CAIs and FUN (fractionation and unknown nuclear isotope anomalies) inclusions, formed early in the inner region of the solar nebula, prior to the injection and homogenization of freshly synthesized short-lived nuclides from a stellar source into this region (Sahijpal and Goswami 1998; Simon et al. 2002; Krot et al. 2008). This model is attractive

and consistent with several petrologic and isotopic observations of  $^{26}\text{Al}$ -free/poor refractory inclusions. Hibonite-bearing CAIs are very refractory and  $^{16}\text{O}$ -enriched, indicating their early formation in the solar nebula. Some hibonite-bearing inclusions have slight depletions of  $^{26}\text{Mg}$ , reflecting an initial Mg anomaly (Ireland et al. 1991; Russell et al. 1998; Simon et al. 1998; Liu et al. 2009). Such a deficit should not be present in samples which postdate the formation of typical CAIs in the solar nebula as the inner solar system is highly homogeneous in the Mg isotope composition (Chakrabarti and Jacobsen 2010). The large stable isotopic anomalies (e.g., Ca and Ti) observed in  $^{26}\text{Al}$ -free/poor hibonite-bearing CAIs strongly support such a scenario. We conclude that  $^{26}\text{Al}$ -free/poor and  $^{26}\text{Al}$ -rich hibonite-bearing CAIs in Ningqiang formed, respectively, before and after injection of  $^{26}\text{Al}$  into the solar nebula from a nearby stellar source.

*Acknowledgments*—The authors thank Steve Simon, Julie Paque, Christine Floss, and one anonymous reviewer for their constructive reviews. This work was supported by Chinese National Natural Science Foundation (grant nos. 40773046, 41003026, 10621303) and by the Minor Planet Foundation of China.

*Editorial Handling*—Dr. Christine Floss

## REFERENCES

- Amelin Y., Krot A. N., Hutcheon I. D., and Ulyanov A. A. 2002. Lead isotopic ages of chondrules and calcium-aluminum-rich inclusions. *Science* 297:1678–1683.
- Boss A. P. and Vanhala H. A. T. 2000. Triggering protostellar collapse, injection, and disk formation. *Space Science Reviews* 92:13–22.
- Busso M., Gallino R., and Wasserburg G. J. 2003. Short-lived nuclei in the early solar system: A low mass stellar source? *Publications of the Astronomical Society of Australia* 20:356–370.
- Cameron A. G. W. and Truran J. W. 1977. The supernova trigger for formation of the solar system. *Icarus* 30:447–461.
- Cameron A. G. W., Hoflich P., Myers P. C., and Clayton D. D. 1995. Massive supernovae, orion gamma rays, and the formation of the solar system. *The Astrophysical Journal Letters* 447:L53–L57.
- Catanzaro E. J., Murphy T. J., Garner E. L., and Shields W. R. 1966. Absolute isotopic abundance ratios and atomic weights of magnesium. *Journal of Research of the National Bureau of Standards* 70a:453–458.
- Chakrabarti R. and Jacobsen S. B. 2010. The isotopic composition of magnesium in the inner solar system. *Earth and Planetary Science Letters* 293:349–358.
- Ciesla F. J. 2010. The distributions and ages of refractory objects in the solar nebula. *Icarus* 208:455–467.
- Connelly J. N., Bizzarro M., Thrane K., and Baker J. 2008. The Pb-Pb age of angrite SAH 99555 revisited. *Geochimica et Cosmochimica Acta* 72:4813–4824.
- Cosarinsky M., Taylor D. J., and McKeegan K. D. 2006. Aluminum-26 model ages of hibonite and spinel from type A inclusions in CV chondrites (abstract #2357). 37th Lunar and Planetary Science Conference. CD-ROM.
- Fahey A. J., Zinner E. K., Crozaz G., and Kornacki A. S. 1987. Microdistributions of Mg isotopes and REE abundances in a type A calcium-aluminum-rich inclusion from Efremovka. *Geochimica et Cosmochimica Acta* 51:3215–3229.
- Foster P. N. and Boss A. P. 1997. Injection of radioactive nuclides from the stellar source that triggered the collapse of the presolar nebula. *The Astrophysical Journal* 489:346–357.
- Gounelle M., Shu F. H., Shang H., Glassgold A. E., Rehm K. E., and Lee T. 2001. Extinct radioactivities and protosolar cosmic rays: Self-shielding and light elements. *The Astrophysical Journal* 548:1051–1070.
- Grossman L. 1972. Condensation in the primitive solar nebula. *Geochimica et Cosmochimica Acta* 36:597–619.
- Guan Y., Huss G. R., MacPherson G. J., and Wasserburg G. J. 2000. Calcium-aluminum-rich inclusions from enstatite chondrites: Indigenous or foreign? *Science* 289:1330–1333.
- Guan Y., Huss G. R., Leshin L. A., MacPherson G. J., and McKeegan K. D. 2006. Oxygen isotope and  $^{26}\text{Al}$ - $^{26}\text{Mg}$  systematics of aluminum-rich chondrules from unequilibrated enstatite chondrites. *Meteoritics & Planetary Science* 41:33–47.
- Guimon R. K., Symes S. J. K., Sears D. W. G., and Benoit P. H. 1995. Chemical and physical studies of type 3 chondrites XII: The metamorphic history of CV chondrites and their components. *Meteoritics* 30:704–714.
- Hinton R. W., Davis A. M., Scatena-Wachel D. E., Grossman L., and Draus R. J. 1988. A chemical and isotopic study of hibonite-rich refractory inclusions in primitive meteorites. *Geochimica et Cosmochimica Acta* 52:2573–2598.
- Hsu W., Wasserburg G. J., and Huss G. R. 2000. High time resolution by use of the Al-26 chronometer in the multistage formation of a CAI. *Earth and Planetary Science Letters* 182:15–29.
- Hsu W., Huss G. R., and Wasserburg G. J. 2003. Al-Mg systematics of CAIs, POI, and ferromagnesian chondrules from Ningqiang. *Meteoritics & Planetary Science* 38:35–48.
- Huss G. R., MacPherson G. J., Wasserburg G. J., Russell S. S., and Srinivasan G. 2001. Aluminum-26 in calcium-aluminum-rich inclusions and chondrules from unequilibrated ordinary chondrites. *Meteoritics & Planetary Science* 36:975–997.
- Huss G. R., Meshik A. P., Smith J. B., and Hohenberg C. M. 2003. Presolar diamond, silicon carbide, and graphite in carbonaceous chondrites: Implications for thermal processing in the solar nebula. *Geochimica et Cosmochimica Acta* 67:4823–4848.
- Hutcheon I. D. and Hutchison R. 1989. Evidence from the Semarkona ordinary chondrite for Al-26 heating of small planets. *Nature* 337:238–241.
- Ireland T. R. 1988. Correlated morphological, chemical, and isotopic characteristics of hibonites from the Murchison carbonaceous chondrite. *Geochimica et Cosmochimica Acta* 52:2827–2839.

- Ireland T. R. 1990. Presolar isotopic and chemical signatures in hibonite-bearing refractory inclusions from the Murchison carbonaceous chondrite. *Geochimica et Cosmochimica Acta* 54:3219–3237.
- Ireland T. R., Fahey A. J., and Zinner E. K. 1991. Hibonite-bearing microspherules—A new type of refractory inclusions with large isotopic anomalies. *Geochimica et Cosmochimica Acta* 55:367–379.
- Jacobsen B., Yin Q., Moynier F., Amelin Y., Krot A. N., Nagashima K., Hutcheon I. D., and Palme H. 2008.  $^{26}\text{Al}$ - $^{26}\text{Mg}$  and  $^{207}\text{Pb}$ - $^{206}\text{Pb}$  systematics of Allende CAIs: Canonical solar initial  $^{26}\text{Al}/^{27}\text{Al}$  ratio reinstated. *Earth and Planetary Science Letters* 272:353–364.
- Kimura M., Noguchi T., Lin Y., and Wang D. 1997. Petrology and mineralogy of an unusual Ningqiang carbonaceous chondrite. In *Geochemical studies on synthetic and natural rock systems*, edited by Gupta A. K., Onuma K., and Arima M. Chennai: Allied Publishers Ltd. pp. 153–165.
- Kita N. T., Nagahara H., Togashi S., and Morishita Y. 2000. A short duration of chondrule formation in the solar nebula: Evidence from  $^{26}\text{Al}$  in Semarkona ferromagnesian chondrules. *Geochimica et Cosmochimica Acta* 64:3913–3922.
- Krot A. N., Meibom A., Weisberg M. K., and Keil K. 2002. Invited review: The CR chondrite clan: Implications for early solar system processes. *Meteoritics & Planetary Science* 37:1451–1490.
- Krot A. N., Hutcheon I. D., Yurimoto H., Cuzzi J. N., McKeegan K. D., Scott E. R. D., Libourel G., Chaussidon M., Ale'ou J., and Petaev M. I. 2005. Evolution of oxygen isotopic composition in the inner solar nebula. *The Astrophysical Journal* 622:1333–1342.
- Krot A. N., Nagashima K., Bizzarro M., Huss G. R., Davis A. M., Meyer B. S., and Ulyanov A. A. 2008. Multiple generations of refractory inclusions in the metal-rich carbonaceous chondrites Acfer 182/214 and Isheyevo. *The Astrophysical Journal* 672:713–721.
- LaTourrette T. and Hutcheon I. D. 1999. Magnesium diffusion in melilite: Thermal histories for CAIs and their parent bodies (abstract #2003). 30th Lunar and Planetary Science Conference. CD-ROM.
- LaTourrette T. and Wasserburg G. J. 1998. Magnesium diffusion in anorthite: Implications for the formation of early solar system planetesimals. *Earth and Planetary Science Letters* 158:91–108.
- Lee T. and Shen J. J. 2001. An X-wind origin for FUN inclusions (abstract). *Meteoritics & Planetary Science* 36:A111.
- Lee T., Papanastassiou D. A., and Wasserburg G. J. 1977.  $^{26}\text{Al}$  in the early solar system: Fossil or fuel? *The Astrophysical Journal Letters* 211:L107–L110.
- Lee T., Shu F. H., Shang H., Glassgold A. E., and Rehm K. E. 1998. Protostellar cosmic rays and extinct radioactivities in meteorites. *The Astrophysical Journal* 506:898–912.
- Liu M., McKeegan K. D., Goswami J. N., Marhas K. K., Sahijpal S., Ireland T. R., and Davis A. M. 2009. Isotopic records in CM hibonites: Implications for time scales of mixing of isotope reservoirs in the solar nebula. *Geochimica et Cosmochimica Acta* 73:5051–5079.
- Lyons J. R. and Young E. D. 2005. CO self-shielding as the origin of oxygen isotope anomalies in the early solar nebula. *Nature* 435:317–320.
- Lyons J. R., Bergin E. A., Ciesla F. J., Davis A. M., Desch S. J., Hashizume K., and Lee J.-E. 2009. Time scales for the evolution of oxygen isotope compositions in the solar nebula. *Geochimica et Cosmochimica Acta* 73:4998–5017.
- MacPherson G. J. 2003. Calcium-aluminum-rich inclusions in chondritic meteorites. In *Meteorites, comets, and planets*, edited by Davis A. M. Treatise on Geochemistry, vol. 1. Oxford: Elsevier-Perigamon. pp. 201–246.
- MacPherson G. J., Davis A. M., and Zinner E. K. 1995. The distribution of aluminum-26 in the early solar system—A reappraisal. *Meteoritics* 30:365–386.
- Mahoney W. A., Ling J. C., Wheaton W. A., and Jacobson A. S. 1984. HEAO 3 discovery of Al-26 in the interstellar medium. *The Astrophysical Journal* 286:578–585.
- Makide K., Nagashima K., Krot A. N., Huss G. R., Hutcheon I. D., and Bischoff A. 2009. Oxygen- and magnesium-isotope compositions of calcium-aluminum-rich inclusions from CR2 carbonaceous chondrites. *Geochimica et Cosmochimica Acta* 73:5018–5050.
- Marhas K. K., Goswami J. N., and Davis A. M. 2002. Short-lived nuclides in hibonite grains from Murchison: Evidence for solar system evolution. *Science* 298:2182–2185.
- Ouellette N., Desch S. J., Bizzarro M., Boss A. P., Ciesla F., and Meyer B. 2009. Injection mechanisms of short-lived radionuclides and their homogenization. *Geochimica et Cosmochimica Acta* 73:4946–4962.
- Russell S. S., Huss G. R., Fahey A. J., Greenwood R. C., Hutcheon R., and Wasserburg G. J. 1998. An isotopic and petrologic study of calcium-aluminum-rich inclusions from CO3 meteorites. *Geochimica et Cosmochimica Acta* 62:689–714.
- Sahijpal S. and Goswami J. N. 1998. Refractory phases in primitive meteorites devoid of  $^{26}\text{Al}$  and  $^{41}\text{Ca}$ : Representative samples of first solar system solids? *The Astrophysical Journal* 509:L137–L140.
- Sahijpal S. and Gupta G. 2009. The plausible source(s) of  $^{26}\text{Al}$  in the early solar system: A massive star or the X-wind irradiation scenario? *Meteoritics & Planetary Science* 44:879–890.
- Sahijpal S., Goswami J. N., Davis A. M., Grossman L., and Lewis R. S. 1998. A stellar origin for the short-lived nuclides in the early solar system. *Nature* 391:559–561.
- Shu F. H., Shang H., and Lee T. 1996. Toward an astrophysical theory of chondrites. *Science* 271:1545–1552.
- Shu F. H., Shang H., Glassgold A. E., and Lee T. 1997. X-rays and fluctuating X-winds from protostars. *Science* 277:1475–1479.
- Simon S. B., Davis A. M., Grossman L., and Zinner E. K. 1998. Origin of hibonite-pyroxene spherules found in carbonaceous chondrites. *Meteoritics & Planetary Science* 33:411–424.
- Simon S. B., Davis A. M., Grossman L., and McKeegan K. D. 2002. A hibonite-coriundum inclusion from Murchison: A first-generation condensate from the solar nebula. *Meteoritics & Planetary Science* 37:533–548.
- Thrane K., Bizzarro M., and Baker J. A. 2006. Extremely brief formation interval for refractory inclusions and uniform distribution of  $^{26}\text{Al}$  in the early solar system. *The Astrophysical Journal* 646:L159–L162.
- Villeneuve J., Chaussidon M., and Libourel G. 2009. Homogeneous distribution of  $^{26}\text{Al}$  in the solar system from the Mg isotopic composition of chondrules. *Science* 325:985–988.

- Wang Y. and Hsu W. 2009. Petrology and mineralogy of the Ningqiang carbonaceous chondrite. *Meteoritics & Planetary Science* 44:763–780.
- Wasserburg G. J., Busso M., Gallino R., and Nollett K. M. 2006. Short-lived nuclei in the early solar system: Possible AGB sources. *Nuclear Physics A* 777:5–69.
- Weidenschilling S. J. and Cuzzi J. N. 1993. Formation of planetesimals in the solar nebula. In *Protostars and planets III*, edited by Levy E. H. and Lunine J. I. Tucson, AZ: The University of Arizona Press. pp. 1031–1060.
- Yurimoto H. and Kuramoto K. 2004. Molecular cloud origin for the oxygen isotope heterogeneity in the solar system. *Science* 305:1763–1766.
- Zhang A. and Hsu W. 2009. Refractory inclusions and aluminum-rich chondrules in Sayh al Uhaymir 290 CH chondrite: Petrography and mineralogy. *Meteoritics & Planetary Science* 44:787–804.
- Zinner E. K., Fahey A. J., McKeegan K. D., Goswami J. N., and Ireland T. R. 1986. Large Ca-48 anomalies are associated with Ti-50 anomalies in Murchison and Murray hibonites. *The Astrophysical Journal* 311:L103–L107.
-